arXiv:1011.2075v1 [nucl-th] 9 Nov 2010

Analysis of three-nucleon forces effects in the $A = 3$ system

A. Kievsky[1]

[1] Istituto Nazionale di Fisica Nucleare, Largo B. Pontecorvo 3, 56127 Pisa, Italy

Abstract. Using modern nucleon-nucleon interactions in the description of the $A = 3, 4$ nuclear systems the χ^2 per datum results to be much bigger than one. In particular it is not possible to reproduce the three- and four-nucleon binding energies and the $n - d$ scattering length simultaneously. This is one manifestation of the necessity of including a three-nucleon force in the nuclear Hamiltonian. In this paper we perform an analysis of some, widely used, three-nucleon force models. We analyze their capability to describe the aforementioned quantities and, to improve their description, we propose modifications in the parametrization of the models. The effects of these new parametrization are studied in some polarization observables at low energies.

1 Introduction

Realistic nucleon-nucleon (NN) potentials reproduce the experimental NN scattering data up to energies of 350 MeV with a χ^2 per datum close to one. However, the use of these potentials in the description of the three- and four-nucleon bound and scattering states gives a χ^2 per datum much bigger than one (see for example Ref. [1]). In order to reproduce correctly the three-nucleon bound state energy, different three-nucleon force (TNF) models have been introduced as the Tucson-Melbourne (TM), Brazil (BR) and the Urbana IX (URIX) models [2, 3, 4]. These models are based on the exchange mechanism of two pions between three nucleons. In the case of the TM model, it has been revisited within a chiral symmetry approach [5], and it has been demonstrated that the contact term present in it should be dropped. This new TM potential, known as TM', has been subsequently readjusted [6] and the final operatorial structure coincides with that one given in the TNF of Brazil. TNF models based on $\pi\rho$ and $\rho\rho$ meson exchange mechanisms have also been derived [7] and their effects have been studied in the triton binding energy [8]. More recently, TNFs have been derived [9] using a chiral effective field theory at next-to-next-to-leading order. A local version of these interactions (hereafter referred as N2LOL) can be found in Ref. [10]. At next-to-next-to-leading order, the TNF has two unknown constants that have

to be determined. It is a common practice to determine these parameters from the three- and four-nucleon binding energies ($B(^3\text{H})$ and $B(^4\text{He})$, respectively). It should be noticed that in this procedure, the three- and four- nucleon systems are described in the framework of the non relativistic quantum mechanics. Relativistic corrections to the few-nucleon binding energies have been studied in Ref. [11] and, recently, the three-nucleon Faddeev equations have been solved in a Poincaré invariant model [12]. These efforts are directed to establish if some of the discrepancies observed between experimental data and theoretical descriptions, as for example the minimum of the $N - d$ differential cross section, can be reduced if relativistic corrections are taken into account.

The $n - d$ doublet scattering length $^2a_{nd}$ is correlated, to some extent, to the $A = 3$ binding energy through the so-called Phillips line [13, 14]. However the presence of TNFs could break this correlation. Therefore $^2a_{nd}$ can be used as an independent observable to evaluate the capability of the interaction models to describe the low energy region. In Ref. [15] results for different combinations of NN interactions plus TNF models are given. We report the results for the quantities of interest in Table I. From the table, we can observe that the models are not able to describe simultaneously the $A = 3, 4$ binding energies and $^2a_{nd}$. In Ref. [16] a comparative study of the aforementioned TNF models has been performed. The AV18 [17] was used as the reference NN interaction and the three-nucleon interaction models were added to it. Different parametrizations of the URIX, TM' and N2LOL TNF have been constructed in order to reproduce, in conjunction with the AV18 interaction, $B(^3\text{H})$, $B(^4\text{He})$ and $^2a_{nd}$. In a second step some polarization observables in $p - d$ scattering at $E_{lab} = 3$ MeV have been studied. In the case of the vector analyzing powers, it was observed that the predictions of the different parametrizations appear in narrow bands with different positions for each model. Compared to the original AV18+URIX model, the results obtained using the parametrizations of the N2LOL model were slightly better, in particular for A_y and iT_{11}. The results obtained using the parametrizations of the TM' were of the same quality. Conversely, the proposed parametrizations for the URIX model produced a much worse description of A_y and iT_{11} than the original URIX model. A possible explanation for this fact is the particular behavior of the profile functions $Y(r)$ and $T(r)$ used in the construction of the model. To this end, in the present paper, we study a different functional form of the profile functions $Y(r)$ and $T(r)$.

2 Three Nucleon Force Models

In Ref. [15] the description of bound states and zero-energy states for $A = 3, 4$ has been reviewed in the context of the HH method. In Table 1 we report results for the triton and ^4He binding energies as well as for the doublet $n - d$ scattering length $^2a_{nd}$ using the AV18 and the N3LO-Idaho [18] NN potentials and using the following combinations of two- and three-nucleon interactions: AV18+URIX, AV18+TM' and N3LO-Idaho+N2LOL. The results are compared to the experimental values of the binding energies and $^2a_{nd}$ [19].

From the table we observe that the results obtained using an interaction

model that includes a TNF are close to the corresponding experimental values. In the case of the AV18+TM', the strength of the TM' potential has been fixed to reproduce the ^{4}He binding energy and the triton binding energy is slightly underpredicted. Conversely, the strength of the URIX potential has been fixed to reproduce the triton binding energy, giving too much binding for ^{4}He. The strength of the N2LOL potential has been fixed to reproduce simultaneously the triton and the ^{4}He binding energies. In the three cases the predictions for the doublet scattering length are not in agreement with the experimental value.

Table 1. The triton and ^{4}He binding energies B (MeV), and doublet scattering length $^2a_{nd}$ (fm) calculated using the AV18 and the N3LO-Idaho two-nucleon potentials, and the AV18+URIX, AV18+TM' and N3LO-Idaho+N2LOL two- and three-nucleon interactions. The experimental values are given in the last row.

Potential	$B(^3\mathrm{H})$	$B(^4\mathrm{He})$	$^2a_{nd}$
AV18	7.624	24.22	1.258
N3LO-Idaho	7.854	25.38	1.100
AV18+TM'	8.440	28.31	0.623
AV18+URIX	8.479	28.48	0.578
N3LO-Idaho+N2LOL	8.474	28.37	0.675
Exp.	8.482	28.30	0.645±0.003±0.007

Following Ref. [16] we give a brief description of the TNF models. Starting from the general form

$$W = \sum_{i<j<k} W(i,j,k) \ , \tag{1}$$

a generic term can be decomposed as

$$W(1,2,3) = aW_a(1,2,3)+bW_b(1,2,3)+dW_d(1,2,3)+c_DW_D(1,2,3)+c_EW_E(1,2,3) \ . \tag{2}$$

Each term corresponds to a different mechanism and has a different operatorial structure. The specific form of these three terms in configuration space is the following:

$$
\begin{aligned}
W_a(1,2,3) &= W_0(\boldsymbol{\tau}_1 \cdot \boldsymbol{\tau}_2)(\boldsymbol{\sigma}_1 \cdot \boldsymbol{r}_{31})(\boldsymbol{\sigma}_2 \cdot \boldsymbol{r}_{23})y(r_{31})y(r_{23}) \\
W_b(1,2,3) &= W_0(\boldsymbol{\tau}_1 \cdot \boldsymbol{\tau}_2)[(\boldsymbol{\sigma}_1 \cdot \boldsymbol{\sigma}_2)y(r_{31})y(r_{23}) \\
&\quad + (\boldsymbol{\sigma}_1 \cdot \boldsymbol{r}_{31})(\boldsymbol{\sigma}_2 \cdot \boldsymbol{r}_{23})(\boldsymbol{r}_{31} \cdot \boldsymbol{r}_{23})t(r_{31})t(r_{23}) \\
&\quad + (\boldsymbol{\sigma}_1 \cdot \boldsymbol{r}_{31})(\boldsymbol{\sigma}_2 \cdot \boldsymbol{r}_{31})t(r_{31})y(r_{23}) \\
&\quad + (\boldsymbol{\sigma}_1 \cdot \boldsymbol{r}_{23})(\boldsymbol{\sigma}_2 \cdot \boldsymbol{r}_{23})y(r_{31})t(r_{23})] \\
W_d(1,2,3) &= W_0(\boldsymbol{\tau}_3 \cdot \boldsymbol{\tau}_1 \times \boldsymbol{\tau}_2)[(\boldsymbol{\sigma}_3 \cdot \boldsymbol{\sigma}_2 \times \boldsymbol{\sigma}_1)y(r_{31})y(r_{23}) \\
&\quad + (\boldsymbol{\sigma}_1 \cdot \boldsymbol{r}_{31})(\boldsymbol{\sigma}_2 \cdot \boldsymbol{r}_{23})(\boldsymbol{\sigma}_3 \cdot \boldsymbol{r}_{31} \times \boldsymbol{r}_{23})t(r_{31})t(r_{23}) \\
&\quad + (\boldsymbol{\sigma}_1 \cdot \boldsymbol{r}_{31})(\boldsymbol{\sigma}_2 \cdot \boldsymbol{r}_{31} \times \boldsymbol{\sigma}_3)t(r_{31})y(r_{23}) \\
&\quad + (\boldsymbol{\sigma}_2 \cdot \boldsymbol{r}_{23})(\boldsymbol{\sigma}_3 \cdot \boldsymbol{r}_{23} \times \boldsymbol{\sigma}_1)y(r_{31})t(r_{23})] \ ,
\end{aligned}
\tag{3}
$$

with W_0 an overall strength. The b- and d-terms are present in the three models whereas the a-term is present in the TM' and N2LOL and not in URIX. Here

we are interested in the profile functions $y(r)$ and $t(r)$. In the first two models these functions are obtained from the following function

$$f_0(r) = \frac{12\pi}{m_\pi^3} \frac{1}{2\pi^2} \int_0^\infty dq q^2 \frac{j_0(qr)}{q^2 + m_\pi^2} F_\Lambda(q) \tag{4}$$

where m_π is the pion mass and

$$y(r) = \frac{1}{r} f_0'(r)$$
$$t(r) = \frac{1}{r} y'(r) \quad . \tag{5}$$

The cutoff function F_Λ in the TM' or Brazil models is taken as $F_\Lambda = [(\Lambda^2 - m_\pi^2)/(\Lambda^2 + q^2)]^2$. In the N2LOL model it is taken as $F_\Lambda = \exp(-q^4/\Lambda^4)$. The momentum cutoff Λ is a parameter of the model fixing the scale of the problem in momentum space. In the N2LOL, it has been fixed to $\Lambda = 500$ MeV, whereas in the TM' model the ratio Λ/m_π has been varied to describe the triton or ^{4}He binding energy at fixed values of the constants a,b and d. In the literature the TM' potential has been used many times with typical values around $\Lambda = 5\, m_\pi$.

In the URIX model the radial dependence of the b- and d-terms is given in terms of the functions

$$Y(r) = e^{-x}/x\, \xi_Y$$
$$T(r) = (1 + 3/x + 3/x^2)Y(r)\, \xi_T \tag{6}$$

with $x = m_\pi r$ and the cutoff functions are defined as $\xi_Y = \xi_T = (1 - e^{-cr^2})$, with $c = 2.1$ fm^{-2}. This regularization has been used in the AV18 potential as well. Since the URIX model has been constructed in conjunction with the AV18 potential, the use of the same regularization was a choice of consistency. The relation between the functions $Y(r), T(r)$ and those of the previous models is:

$$Y(r) = y(r) + T(r)$$
$$T(r) = \frac{r^2}{3} t(r) \quad . \tag{7}$$

With the definition given in Eq.(4), the asymptotic behavior of the functions $f_0(r)$, $y(r)$ and $t(r)$ is:

$$f_0(r \to \infty) \to \frac{3}{m_\pi^2} \frac{e^{-x}}{x}$$
$$y(r \to \infty) \to -\frac{3e^{-x}}{x^2}\left(1 + \frac{1}{x}\right) \tag{8}$$
$$t(r \to \infty) \to \frac{3}{r^2} \frac{e^{-x}}{x}\left(1 + \frac{3}{x} + \frac{3}{x^2}\right) \quad .$$

To be noticed that with the normalization chosen for f_0, the functions Y and T defined from y and t and those ones defined in the URIX model coincide at large separation distances.

The last two terms in Eq.(2) correspond to a two-nucleon (2N) contact term with a pion emitted or absorbed (D-term) and to a three-nucleon (3N) contact interaction (E-term). Their local form, in configuration space, derived in Ref. [10], is

$$
\begin{aligned}
W_D(1,2,3) = W_0^D(\boldsymbol{\tau}_1 \cdot \boldsymbol{\tau}_2)\{&(\boldsymbol{\sigma}_1 \cdot \boldsymbol{\sigma}_2)[y(r_{31})Z_0(r_{23}) + Z_0(r_{31})y(r_{23})] \\
&+ (\boldsymbol{\sigma}_1 \cdot \boldsymbol{r}_{31})(\boldsymbol{\sigma}_2 \cdot \boldsymbol{r}_{31})t(r_{31})Z_0(r_{23}) \\
&+ (\boldsymbol{\sigma}_1 \cdot \boldsymbol{r}_{23})(\boldsymbol{\sigma}_2 \cdot \boldsymbol{r}_{23})Z_0(r_{31})t(r_{23})\} \\
W_E(1,2,3) = W_0^E(\boldsymbol{\tau}_1 \cdot \boldsymbol{\tau}_2)&Z_0(r_{31})Z_0(r_{23}) \ .
\end{aligned}
\tag{9}
$$

The constants W_0^D and W_0^E fix the strength of these terms. In the case of the URIX model the D-term is absent whereas the E-term is present without the isospin operatorial structure and it has been included as purely phenomenological, without justifying its form from a particular exchange mechanism. Its radial dependence has been taken as $Z_0(r) = T^2(r)$. In the N2LOL model, the function $Z_0(r)$ is defined as

$$
Z_0(r) = \frac{12\pi}{m_\pi^3} \frac{1}{2\pi^2} \int_0^\infty dq q^2 j_0(qr) F_\Lambda(q)
\tag{10}
$$

with the same cutoff function used before, $F_\Lambda(q) = \exp(-q^4/\Lambda^4)$. In the TM' model the D- and E-terms are absent.

In order to analyze the different short range structure of the TNF models, in Fig. 1 we compare the dimensionless functions $Z_0(r)$, $y(r)$ and $T(r)$ for the three models under consideration. In the TM' model using the definition of Eq.(10) and using the corresponding cutoff function we can define:

$$
Z_0^{TM}(r) = \frac{12\pi}{m_\pi^3} \frac{1}{2\pi^2} \int_0^\infty dq q^2 j_0(qr) \left(\frac{\Lambda^2 - m_\pi^2}{\Lambda^2 + q^2}\right)^2 = \frac{3}{2}\left(\frac{m_\pi}{\Lambda}\right)\left(\frac{\Lambda^2}{m_\pi^2} - 1\right)^2 e^{-\Lambda r} \ .
\tag{11}
$$

This function is shown in the first panel of Fig. 1 as a dashed line. From the figure we can see that, in the case of the URIX model, the functions $Z_0(r)$ and $y(r)$ go to zero as $r \to 0$. This is not the case for the other two models and is a consequence of the choice to regularize the Y and T functions adopted in the URIX. The function $Z_0^{TM}(r)$ has been introduced in Ref. [16] to add a repulsive term to the TM' model. In fact, it was shown that without it, the AV18+TM' model was unable to reproduce simultaneously the triton binding energy and the doublet scattering length for reasonable values of the TM' strength parameters.

3 Parametrization of the profile functions $Z_0(r)$, $y(r)$ and $T(r)$

In this section we study a possible parametrization of the profile functions $Z_0(r)$, $y(r)$ and $T(r)$. The function Z_0 is defined in Eq.(10), its behavior for small values of r can be derived from the expansion of the Bessel function as

$$
Z_0(r \to 0) = \frac{12\pi}{m_\pi^3} \frac{1}{2\pi^2} \int_0^\infty dq q^2 \left[1 - \frac{q^2 r^2}{6} + \dots\right] F_\Lambda(q)
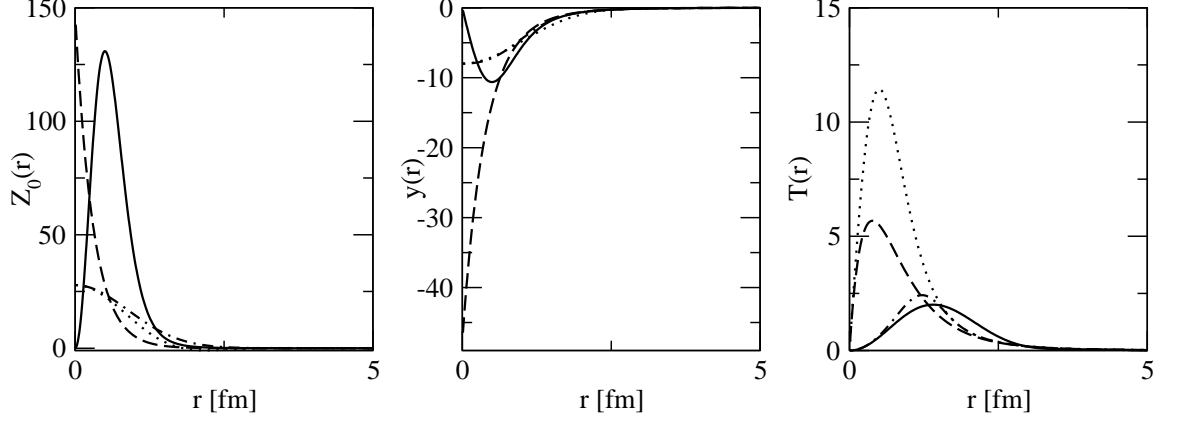\tag{12}
$$

Figure 1. The $Z_0(r)$, $y(r)$ and $T(r)$ functions as functions of the interparticle distance r for the URIX (solid line), TM' (dashed line) and N2LOL (dotted line) models. The dotte-dashed line shows the one-parameter functions defined in Eqs.(14) and (16).

For a sharp cutoff this integral can be approximated as

$$Z_0(r \to 0) \approx \frac{12}{m_\pi^3} \frac{1}{2\pi} \left[\frac{\Lambda^3}{3} - r^2 \frac{\Lambda^5}{30} + \ldots \right] \approx \frac{2}{\pi} \left(\frac{\Lambda^3}{m_\pi^3} \right) \left[1 - \frac{r^2 \Lambda^2}{10} \right] \tag{13}$$

Therefore in the following we propose the one-parameter form of the function

$$Z_0(r) = Z_0(0) e^{-r^2 \Lambda^2 / 10} \tag{14}$$

where $Z_0(0)$ can be taken from Eq.(10) using a particular form of cutoff. In the case of sharp cutoff it results: $Z_0(0) = \frac{2}{\pi} \left(\frac{\Lambda^3}{m_\pi^3} \right)$.

The functions $y(r)$ and $t(r)$ are defined in Eq.(5). Their short range behavior, after expanding the corresponding Bessel function, are

$$
\begin{aligned}
y(r \to 0) &= -\frac{12\pi}{m_\pi^3} \frac{1}{2\pi^2} \frac{1}{r} \int_0^\infty dq q^3 \left[\frac{qr}{3} (1 - \frac{q^2 r^2}{10} + \ldots) \right] \frac{F_\Lambda(q)}{q^2 + m_\pi^2} \\
&= y(0) + \frac{1}{2} r^2 t(0) + \ldots \\
t(r \to 0) &= -\frac{12\pi}{m_\pi^3} \frac{1}{2\pi^2} \frac{1}{r^2} \int_0^\infty dq q^4 \left[\frac{q^2 r^2}{15} (1 - \frac{q^2 r^2}{14} + \ldots) \right] \frac{F_\Lambda(q)}{q^2 + m_\pi^2} \\
&= t(0) - \frac{1}{2} r^2 t_2 + \ldots
\end{aligned}
\tag{15}
$$

where we have introduced the corresponding values at $r = 0$ and the quantity t_2 in the second term of $t(r)$. In Eq.(8) the asymptotic behavior of the functions $y(r)$ and $t(r)$ are given. Recalling that $3T(r) = r^2 t(r)$ and considering the short-range behavior indicated above, we will analyze the following one-parameter r-space

form of the functions y and T

$$y(r) = -\frac{3\mathrm{e}^{-x}}{x^2}\left(1 + \frac{1}{x}\right)\left(1 - \mathrm{e}^{-x^3|y(0)|/3}\right)$$

$$T(r) = \frac{\mathrm{e}^{-x}}{x}\left(1 + \frac{3}{x} + \frac{3}{x^2}\right)\left(1 - \mathrm{e}^{-x^3 r^2|t(0)|/9}\right)$$

(16)

These functions are shown in Fig. 1 with the dot-dashed line. They have been calculated using the cutoff of the N2LOL model. As expected they are close to the profile functions of the N2LOL potential. Calculations in the $A = 3$ systems using these profile r-space functions are analyzed in the next section.

4 Results in the $A = 3$ system

In the previous section we have presented the one-parameter profile functions, $Z_0(r)$, $y(r)$ and $T(r)$, obtained from a regularization of their asymptotic form. The regularization was perfomed in order to match the short range behavior of the profile functions defined in the N2LOL potential. As it is shown explicitly in Fig. 1, these functions are very different from those defined in the Urbana potential in which a different regularization was used. In order to study the sensitivity in the description of the $A = 3$ system to different profile functions, we construct a modification of the Urbana model in which the profile functions defined in Eqs.(14) and (16) are used in place of the original ones. The parameters $Z_0(0)$, $y(0)$ and $t(0)$ are calculated using the cutoff of the N2LOL model, $F_\Lambda = \exp(-q^4/\Lambda^4)$, with $\Lambda = 500$ MeV. As mentioned, in the URIX model, only the b-, d and E-terms are included. The corresponding strengths are fixed by the constants $A_{2\pi}^{PW}$, $D_{2\pi}^{PW}$ and A_R. Their original values are shown in the first row of Table 2. Changing the form of the profile functions the values of the constants has to be fixed. Three sets of values, selected to reproduce the triton binding energy and $^2a_{nd}$, are given in Table 2 together with some mean values calculated from the triton wave function.

Table 2. Mean values of the triton kinetic energy, the two-nucleon potential energy $V(2N)$, and the attractive, $V_A(3N)$, and repulsive, $V_R(3N)$, contributions of the TNF to the triton binding energy using the AV18+URIX potential for the specified values of the parameters. In the last column $^2a_{nd}$ is given.

$A_{2\pi}^{PW}$ [MeV]	$D_{2\pi}^{PW}$	A_R [MeV]	T [MeV]	$V(2N)$ [MeV]	$V_A(3N)$ [MeV]	$V_R(3N)$ [MeV]	$^2a_{nd}$ [fm]
-0.0293	0.25	0.0048	51.259	-58.606	-1.126	1.000	0.578
-0.1200	0.25	0.0108	50.110	-57.360	-1.747	0.525	0.643
-0.1200	0.50	0.0155	50.193	-57.328	-2.097	0.759	0.645
-0.1200	0.75	0.0229	50.331	-57.211	-2.735	1.143	0.644

From the table we can observe that with the proposed parametrization the attractive part of the TNF is bigger and, due to the fact that the profile functions are smoother, there is a reduction of the mean value of the kinetic energy. In order to extend further the analysis, $p - d$ scattering observables at $E_{lab} = 3$

MeV have been calculated using the three sets of constants and the new form of the profile functions. The results for the differential cros section, the vector analyzing powers A_y and iT_{11} and the tensor analyzing powers T_{20}, T_{21} and T_{22}, are shown in Fig.2 and compared to the predictions of the original URIX model and the experimental data. From the figure we can observe that, besides a small improvement in A_y and iT_{11}, all the models describe the data with similar quality. However only the models with the profile functions of Eqs.(14) and (16) reproduce the experimental value of $^2a_{nd}$. The fact that the vector analyzing powers improve very little with the new parametrization can be taken as a further evidence that the spin-isospin structure of the URIX is incomplete and different forms could in principle be included [21].

5 Conclusions

Due to the fact that some of the widely used TNF models do not reproduce simultaneously the triton and ^{4}He binding energies and the $n - d$ doublet scattering length, possible modifications of their parametrizations have been analyzed. To this end we have used the AV18 as the reference NN interaction and we have analyze possible modifications of the URIX model. We have modified the regularization of the profile functions $Y(r)$ and $T(r)$ at the origin and we have introduced the $Z_0(r)$ function in the central repulsive E-term. We have used one-parameter functions that have been chosen to match the short-range behavior of the corresponding functions in the N2LOL model. Furthermore the strengths of the b-, d-terms and E-terms have been fixed to reproduce the triton binding energy and $^2a_{nd}$. Then the predictions for some selected scattering observables in $p - d$ scattering at 3 MeV have been compared to the results of the original model and the experimental data. We can observe that the description using the new parametrizations has the same quality of the original model. However, with the proposed parametrizations, the AV18+URIX model describes correctly $B(^3\text{H})$ and $^2a_{nd}$. This analysis can be consider as a preliminary step in a study directed to determine the parametrizations of the profile functions inside the three-body force from the experimental data. Investigations in this direction are underway.

References

1. A. Kievsky, M. Viviani, and S. Rosati, Phys. Rev. C **64**, 024002 (2001)

2. S.A. Coon and W. Glöckle, Phys. Rev. C **23**, 1790 (1981)

3. H.T. Coelho, T.K. Das, and M.R. Robilotta, Phys. Rev. C **28**, 1812 (1983); M.R. Robilotta and H.T. Coelho, Nucl. Phys. A **460**, 645 (1986)

4. B.S. Pudliner, V. R. Pandharipande, J. Carlson, and R.B. Wiringa, Phys. Rev. Lett. **74**, 4396 (1995)

5. J.L. Friar, D. Hüber, and U. van Kolck, Phys. Rev. C **59**, 53 (1999)

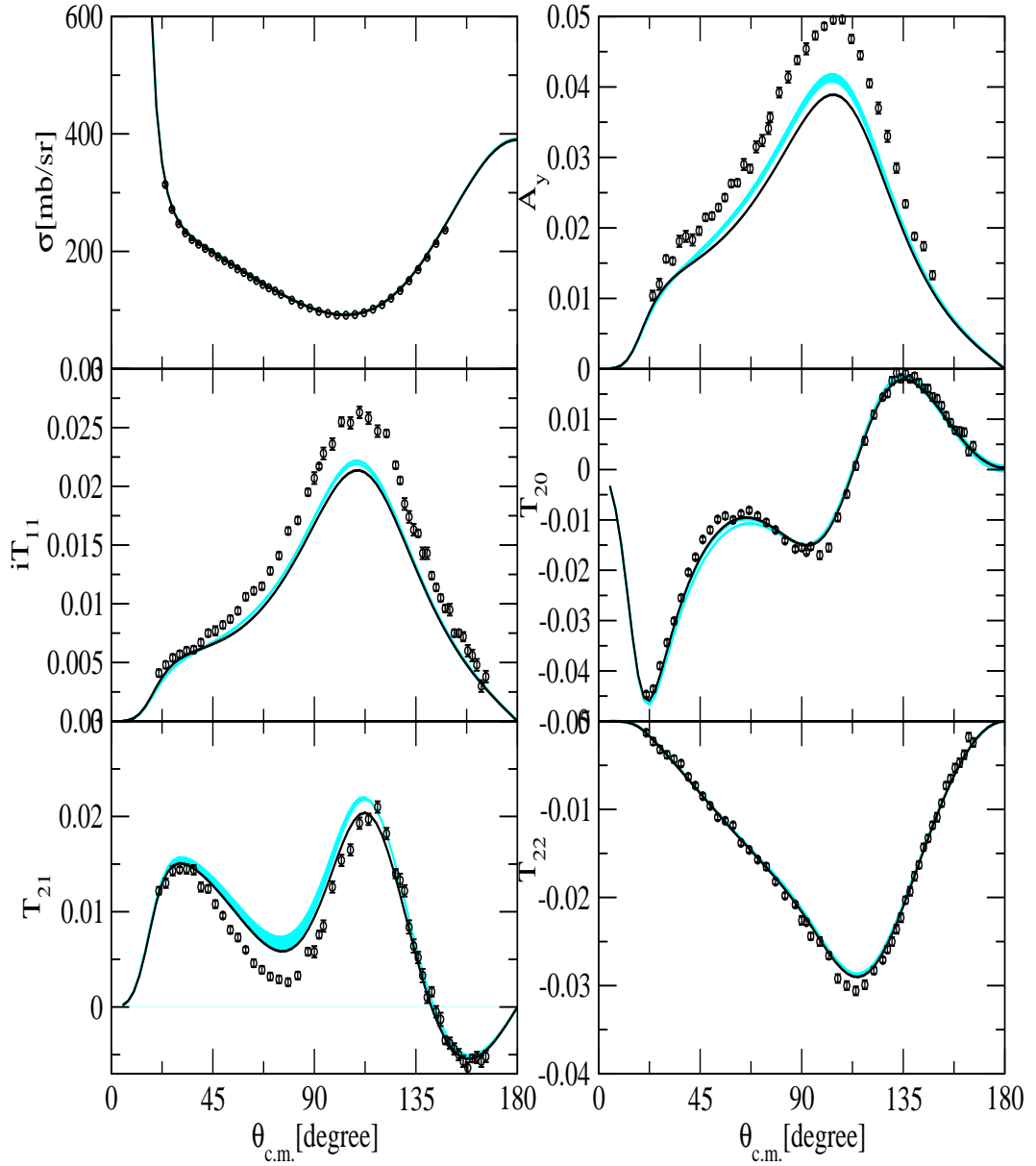6. S.A. Coon and H.K. Han, Few-Body Syst. **30**, 131 (2001)

Figure 2. (Color on line) Differential cross section and vector and tensor polarization observables at $E_{lab} = 3$ MeV using the AV18+URIX model with the parameters given in Table 2 (cyan band). The predictions of the original AV18+URIX model, given in the first row of the table, are shown as a solid line. The experimental points from Ref. [20] are also shown.

7. S.A. Coon and M.T. Peña, Phys. Rev. C **48**, 2559 (1993)

8. A. Stadler, J. Adam, Jr., H. Henning, and P.U. Sauer, Phys. Rev. C **51**, 2896 (1995)

9. E. Epelbaum *et al.*, Phys. Rev. C **66**, 064001 (2002)

10. P. Navratil, Few-Body Syst. **41**, 117 (2007)

11. S.C. Pieper, V.R. Pandharipande, R.B. Wiringa and J. Carlson, Phys. Rev. C **64**, 014001 (2001)

12. H. Witała, J. Golak, W. Glöckle, and H. Kamada, Phys. Rev. C **71**, 054001 (2005)

13. A.C. Phillips, Nucl. Phys. A **107**, 209 (1968)

14. P.F. Bedaque, H.-W. Hammer, and U. van Kolck, Nucl. Phys. A **646**, 444 (1999)

15. A. Kievsky, S. Rosati, M. Viviani, L.E. Marcucci, and L. Girlanda, J. Phys. G: Nucl. Part. Phys. **35**, 063101 (2008)

16. A. Kievsky, M. Viviani, L. Girlanda and L.E. Marcucci, Phys. Rev. C **81**, 044003 (2010)

17. R.B. Wiringa, V.G.J. Stoks, and R. Schiavilla, Phys. Rev. C **51** 38 (1995)

18. D.R. Entem and R. Machleidt, Phys. Rev. C **68** 041001(R) (2003)

19. K. Schoen *et al.*, Phys. Rev. C **67**, 044005 (2003)

20. S. Shimizu *et al.*, Phys. Rev. C **52**, 1193 (1995)

21. A. Kievsky, Phys. Rev. C **60**, 034001 (1999)